

There is a broad spectrum of diagnoses of bilateral lesions in the basal ganglia in the pediatric population. The main causes cited are hypoxic-ischemic encephalopathy; hypoglycemia; encephalitis; inborn errors of metabolism; water and electrolyte disturbances; carbon monoxide poisoning; and demyelinating disorders. The correlation with clinical and laboratory data is fundamental for making the definitive diagnosis^(7,12,13).

In conclusion, the possibility of acute or chronic kernicterus should be considered when clinical symptoms, biochemical data, and MRI findings are suggestive of the disease, the chronic presentation and permanent, irreversible profile being promoted by bilirubin neurotoxicity.

REFERENCES

1. Alfenas R, Niemeyer B, Bahia PRV, et al. Parry-Romberg syndrome: findings in advanced magnetic resonance imaging sequences – case report. *Radiol Bras.* 2014;47:186–8.
2. Bimbato EM, Carvalho AG, Reis F. Toxic and metabolic encephalopathies: iconographic essay. *Radiol Bras.* 2015;48:121–5.
3. Castro FD, Reis F, Guerra JGG. Intraventricular mass lesions at magnetic resonance imaging: iconographic essay – part 1. *Radiol Bras.* 2014;47:176–81.
4. Ono SE, Carvalho Neto A, Gasparetto EL, et al. X-linked adrenoleukodystrophy: correlation between Loes score and diffusion tensor imaging parameters. *Radiol Bras.* 2014;47:342–9.
5. Barbosa JHO, Santos AC, Salmon CEG. Susceptibility weighted imaging: differentiating between calcification and hemosiderin. *Radiol Bras.* 2015;48:93–100.

6. Turkel SB, Miller CA, Guttenberg ME, et al. A clinical pathologic reappraisal of kernicterus. *Pediatrics.* 1982;69:267–72.
7. Parashari UC, Singh R, Yadav R, et al. Changes in the globus pallidus in chronic kernicterus. *J Pediatr Neurosci.* 2009;4:117–9.
8. Perlstein MA. The late clinical syndrome of posticteric encephalopathy. *Pediatr Clin North Am.* 1960;7:665–87.
9. Martich-Kriss V, Kollias SS, Ball WS Jr. MR findings in kernicterus. *AJNR Am J Neuroradiol.* 1995;16(4 Suppl):819–21.
10. Coskun A, Yikilmaz A, Kumandas S, et al. Hyperintense globus pallidus on T1-weighted MR imaging in acute kernicterus: is it common or rare? *Eur Radiol.* 2005;15:1263–7.
11. Govaert P, Lequin M, Swarte R, et al. Changes in globus pallidus with (pre)term kernicterus. *Pediatrics.* 2003;112(6 Pt 1):1256–63.
12. Hegde AN, Mohan S, Lath N, et al. Differential diagnosis for bilateral abnormalities of the basal ganglia and thalamus. *Radiographics.* 2011;31:5–30.
13. Khanna PC, Iyer RS, Chaturvedi A, et al. Imaging bithalamic pathology in the pediatric brain: demystifying a diagnostic conundrum. *AJR Am J Roentgenol.* 2011;197:1449–59.

Bruno Niemeyer de Freitas Ribeiro¹, Gabriela de Almeida Lima¹, Nina Ventura¹, Emerson Leandro Gasparetto¹, Edson Marchiori²

1. Instituto Estadual do Cérebro Paulo Niemeyer, Rio de Janeiro, RJ, Brazil. 2. Universidade Federal do Rio de Janeiro (UFRJ), Rio de Janeiro, RJ, Brazil. Mailing address: Dr. Bruno Niemeyer de Freitas Ribeiro. Instituto Estadual do Cérebro Paulo Niemeyer – Departamento de Radiologia. Rua do Rezende, 156, Centro. Rio de Janeiro, RJ, Brazil, 20231-092. E-mail: bruno.niemeyer@hotmail.com.

<http://dx.doi.org/10.1590/0100-3984.2015.0190>

Renal lymphangiectasia: know it in order to diagnose it

Dear Editor,

Here, we report the case of a 9-year-old girl with hyperparathyroidism. Ultrasound showed renal cysts and increased echogenicity of the parenchyma in both kidneys. The diagnostic hypothesis was hyperparathyroidism secondary to chronic/polycystic kidney disease. The patient presented with gradually worsening kidney function and hypertension, and new imaging scans were requested. The ultrasound showed anechoic, multiloculated images in the pyelocaliceal region of both kidneys, and perirenal, subcapsular cysts. A computed tomography (CT) scan was acquired, although no contrast agent was used, which precluded an accurate characterization. Nevertheless, the CT scan revealed changes similar to those observed on ultrasound. We also performed magnetic resonance imaging (MRI), which showed pyelocaliceal, perirenal cysts, with altered intensity of the signal of the renal parenchyma and loss of corticomedullary differentiation (Figure 1A), confirming, in conjunction with the clinical and biochemical data, the diagnosis of renal lymphangiectasia (RL).

RL is a rare benign disease that occurs because of miscommunication between the renal lymphatic drainage system and the retroperitoneal lymphatic system⁽¹⁾. As a result, there is accumulation of lymph in the renal lymph ducts, making them ectatic and forming simple or multiloculated, typically asymmetric and bilateral, collections in the pyelocaliceal, perinephric, or parenchymal regions, although, in some cases, only a part of one kidney is affected (Figure 1—B,C). There is no predilection for a given gender or age group. As of 2005, only 40 cases had been described^(1,2).

In most cases, RL is an incidental finding, with or without signs and symptoms of pain, increased abdominal volume, hematuria, ascites, edema of the lower limbs, hypertension, erythrocytosis with renal vein thrombosis, and, rarely, chyluria⁽³⁾. Such manifestations can be explained by the distention of the renal

fascia and compression of the renal parenchyma by cysts, fistulization to the pelvic cavity, and changes in the renin-angiotensin system^(2–4). In rare cases, chronic kidney disease has been reported⁽⁵⁾. To our knowledge, there have been no specific reports of clinical evolution to hyperparathyroidism, although a relationship with chronic kidney disease can be assumed.

A CT scan can reveal expansive perirenal formations with fluid attenuation, bounded by the renal fascia, that conform to

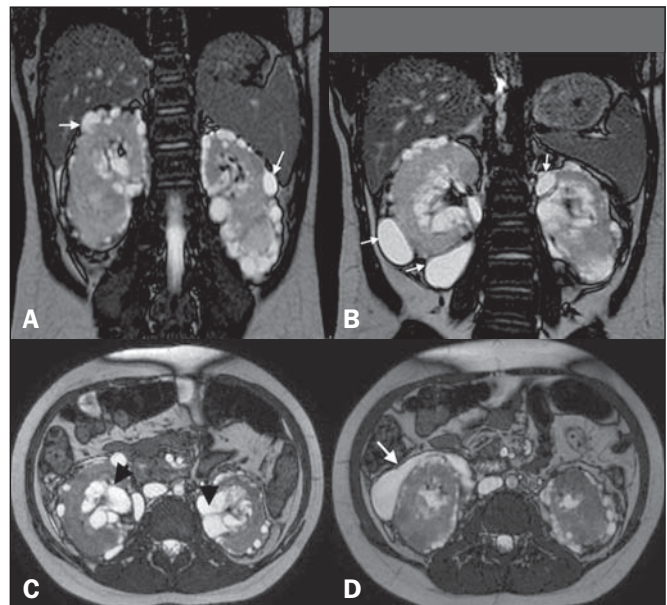


Figure 1. A: Coronal T2-weighted MRI sequence showing a loss of corticomedullary differentiation in both kidneys and multiple cystic lesions, with thin walls, located in the cortex (arrows). **B:** Cystic formations in the subcapsular cortex (arrows). **C:** Axial T2-weighted MRI sequence showing cysts located in the renal sinuses (arrowheads) and perinephric spaces, simulating pelvic dilatation. **D:** The same images simulating cystic collections in the subcapsular cortex (arrow).

(and do not invade) the adjacent structures. Those formations can compress the kidney cortex, expand the sinus and distort the calyceal system. In some cases, small, predominantly peripheral, hypodense collections can be seen, with attenuation values of 0–15 HU⁽³⁾. There may be thickening of the renal fasciae and retroperitoneal collections crossing the midline at the level of the renal hilum. After the administration of iodine contrast, there is no enhancement of the collections or of the walls of the cystic formations⁽⁶⁾. In MRI, the cysts exhibit a low signal on T1-weighted sequences—although the signal strength can be increased if there is bleeding⁽⁶⁾—and a more intense signal on T2-weighted sequences, without enhancement. In addition, RL can be diagnosed on MRI scans by identifying perirenal lymphatic collections with inversion of the corticomedullary signal intensity^(1,4), as depicted in Figure 1—B,C,D.

To suggest a diagnosis of RL, as well as to devise a treatment strategy and to prevent complications, it is essential to understand the radiological aspects of the disease and to differentiate it from other conditions that mimic cystic kidney disease. Although the combination of RL and renal failure is rare, knowledge of that association is also important to prevent comorbid conditions that can evolve with this complication, such as obesity and high blood pressure.

REFERENCES

1. Rastoji R, Rastogi V. Computed tomographic scan in the diagnosis of bilateral renal lymphangiectasia. *Saudi J Kidney Dis Transpl.* 2008;19: 976–9.
2. Ashraf K, Raza SS, Ashraf O, et al. Renal lymphangiectasia. *Br J Radiol.* 2007;80:e117–8.
3. Vega J, Santamarina M. Linfangiectasia renal unilateral. Caso clínico. *Rev Méd Chile.* 2012;140:1312–5.
4. Restrepo JM, Amaya JEL, Sepúlveda NA, et al. Renal lymphangiectasia: MDCT and MRI findings. *Rev Colomb Radiol.* 2011;22:1–8.
5. Ueda S, Yanagida H, Sugimoto K, et al. Chronic renal insufficiency in a boy with cystic renal lymphangiectasia: morphological findings and long-term follow-up. *Clin Nephrol.* 2007;68:416–21.
6. Vasconcelos RA, Pereira ES, Bauab Jr T, et al. Renal lymphangiectasia: incidental finding at multislice computed tomography and literature review. *Radiol Bras.* 2012;45:178–80.

Andréa Farias de Melo Leite¹, Bruna Venturieri¹, Rosana Gonçalves de Araújo¹, Eduardo Just Costa e Silva¹, Jorge Elias Junior²

1. Instituto de Medicina Integral Professor Fernando Figueira de Pernambuco (IMIP), Recife, PE, Brazil. 2. Faculdade de Medicina de Ribeirão Preto da Universidade de São Paulo (FMRP-USP), Ribeirão Preto, SP, Brazil. Mailing address: Dra. Andréa Farias de Melo Leite. Rua Laura Campelo, 130, Torre. Recife, PE, Brazil, 50710-270. E-mail: andreaarias@gmail.com.

<http://dx.doi.org/10.1590/0100-3984.2015.0025>

Primary undifferentiated sarcoma in the thorax: a rare diagnosis in young patients

Dear Editor,

A 30-year-old man was admitted to the thoracic surgery department of a tertiary hospital for investigation of a thoracic mass. Having previously received treatment for pneumonia, he presented with a two-week history of progressively increasing pain in the right hemithorax and right flank, between the anterior axillary line and midaxillary line. On clinical examination, there was an absence of breath sounds in the right hemithorax.

Computed tomography (CT) of the chest showed an extensive, heterogeneous, mostly solid mass in right thoracic region (Figure 1), with areas of inner content of low attenuation (21–26 Hounsfield units) and foci of bleeding, without intervening calcifications and without osteolysis of the rib. Laboratory tests produced results within the limits of normality. The patient underwent percutaneous biopsy, and the pathology examination revealed undifferentiated sarcoma (Figure 2).

Sarcomas represent a heterogeneous group of tumors derived from mesenchymal cells^(1–3). They account for 1% of all neoplasms and occur mainly in the extremities (in 60% of cases), gastrointestinal tract (in 25%), retroperitoneal space (in 20%), and the head and neck region (in 4.1%). Primary sarcomas of the thorax are exceptionally rare, accounting for only 0.2% of lung cancers and only 5% of all the thoracic neoplasms. Such sarcomas can involve the lungs, mediastinum, pleura, and, mainly, the chest wall. The presence of sarcoma in any other part of the body must be ruled out, because metastasis to the chest is much more common than is primary sarcoma of the thorax^(4–7).

The most common histological types of primary sarcomas are angiosarcoma, leiomyosarcoma, rhabdomyosarcoma, and sarcomatoid mesothelioma⁽⁸⁾. In the chest wall, the most common primary sarcomas are Ewing’s sarcoma, primitive neuroectodermal tumor, malignant fibrous histiocytoma, chondrosarcoma, osteosarcoma, synovial sarcoma, and fibrosarcoma⁽⁸⁾. Radiologically, these tumors typically present as large, heterogeneous masses. However, their appearance can vary from an intrabronchial

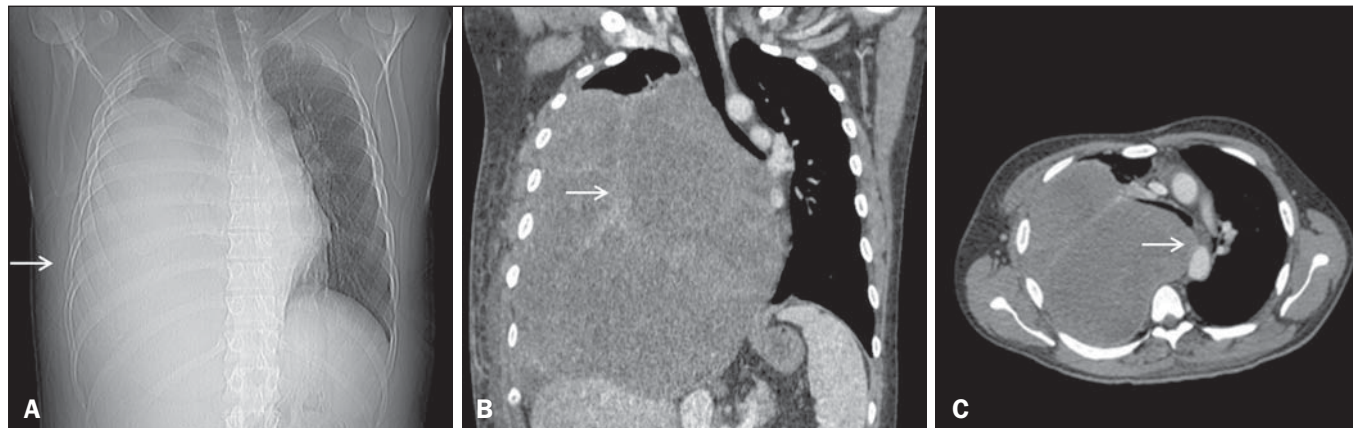


Figure 1. CT scan showing a primary sarcoma in the right hemithorax. **A:** CT scout image showing opacification of the right hemithorax. **B:** Coronal CT reconstruction with heterogeneous enhancement (arrow). **C:** Axial CT slice showing contralateral mediastinal deviation.